N-methyladenosine reader YTHDF2-mediated AC026691.1 degradation promotes gastric cancer cell proliferation, migration and M2 macrophage polarization

CONG-FEI JI[1,2*], JIN-FENG JI[3*], XIAO-BING YU[4] and ZHEN-XIN WANG[5]

[1]Department of Oncology, The First Affiliated Hospital of Soochow University, Suzhou, Jiangsu 215006, P.R. China; [2]Department of Oncology, Affiliated Tumor Hospital of Nantong University, Nantong, Jiangsu 226006, P.R. China; [3]Department of Integrative Chinese and Western Medicine, Affiliated Tumor Hospital of Nantong University, Nantong, Jiangsu 226006, P.R. China; [4]Department of Medical Oncology, The Affiliated Cancer Hospital of Nanjing Medical University, Nanjing, Jiangsu 210009, P.R. China; [5]Department of Medical Oncology, The First Affiliated Hospital of Soochow University, Suzhou, Jiangsu 215006, P.R. China

Received April 28, 2024; Accepted January 3, 2025

DOI: 10.3892/mmr.2025.13485

Abstract. The present study aimed to explore the effects of key N6-methyladenosine (m6A)-related long non-coding RNAs (lncRNAs) on the malignant behavior and macrophage polarization of gastric cancer cells, and their preliminary mechanisms. Gastric cancer-related lncRNA datasets were downloaded from The Cancer Genome Atlas database, and m6A-related differentially expressed lncRNAs (DElncRNAs) were analyzed. Subsequently, Cox regression and lasso regression analyses were used to screen the m6A-related DElncRNAs associated with the prognosis of patients with gastric cancer. Additionally, reverse transcription-quantitative polymerase chain reaction (qPCR) was employed to detect the expression levels of m6A-related lncRNAs in normal gastric epithelial cells (GES-1) and human gastric cancer cells (AGS and MKN-45). In addition, the methylation levels of lncRNAs were measured using a methylated RNA immunoprecipitation qPCR assay kit, and the interaction between m6A-related lncRNAs and m6A-related proteins was observed by RNA pull-down assay. Subsequently, m6A-related lncRNAs and proteins were knocked down separately or simultaneously in gastric cancer cell lines. Bioinformatics analysis revealed that m6A-related AC026691.1 was significantly associated with the prognosis of patients with gastric cancer and had a potential binding site for YT521-B homology domain family member 2 (YTHDF2). The RNA pull-down assay indicated that YTHDF2 not only had binding sites with AC026691.1 but could also markedly promote the degradation of m6A-related AC026691.1. Furthermore, AC026691.1 was lowly expressed in gastric cancer cells, whereas YTHDF2 was highly expressed. Knockdown of YTHDF2 inhibited the proliferation, migration and epithelial-mesenchymal transition of gastric cancer cells, and reduced M2 macrophage polarization. By contrast, knocking down AC026691.1 showed the opposite trend. Knockdown of YTHDF2 and AC026691.1 further confirmed the stable impact of YTHDF2 on AC026691.1. In conclusion, the degradation of AC026691.1 modified by YTHDF2-mediated m6A may promote gastric cancer cell proliferation, migration, epithelial-mesenchymal transition and M2 macrophage polarization.

Correspondence to: Dr Zhen-Xin Wang, Department of Medical Oncology, The First Affiliated Hospital of Soochow University, 188 Shizi Street, Suzhou, Jiangsu 215006, P.R. China
E-mail: zhenxw316@163.com

*Contributed equally

Abbreviations: m6A, N6-methyladenosine; lncRNA, long non-coding RNA; YTHDF2, YT521-B homology domain family member 2; TCGA, The Cancer Genome Atlas; DElncRNAs, differentially expressed lncRNAs; RT-qPCR, reverse transcription-quantitative polymerase chain reaction; EMT, epithelial-mesenchymal transition

Key words: gastric cancer, proliferation, M2 macrophage polarization, YTHDF2, AC026691.1

Introduction

Gastric cancer has long been known as a malignant tumor that poses a severe threat to global human health, and it is one of the most prevalent malignancies of the digestive tract (1). According to global statistics, there are ~600,000 new cases of gastric cancer in men and ~330,000 cases in women annually (2). Moreover, patients with gastric cancer frequently have a poor prognosis, and gastric cancer has the second highest mortality rate among malignant diseases (2). Despite continuous improvements in various diagnostic methods, surgical techniques and chemotherapy regimens for gastric cancer, the 5-year survival rate for patients with gastric cancer remains at 20-30%, and the mortality rate continues to rise (3). The recurrence and metastasis of gastric cancer after surgery are current challenges in the medical field (4). Notably, cell proliferation and migration are pivotal features in the development of cancer, which are closely related to the poor prognosis of patients with

malignant tumors (5). Furthermore, macrophages, a crucial component of tumor-infiltrating immune cells, serve a vital role in tumorigenesis; in particular, M2 macrophages have been demonstrated to contribute to the growth and progression of gastric cancer (6). Previously, Zhan *et al* (7) identified key molecules and mechanisms affecting the development of gastric cancer; however, further research is still required.

Long non-coding RNA (lncRNA) is a well-recognized non-coding form of RNA with a length of >200 nucleotides (8). Numerous studies have reported the involvement of non-coding RNAs in gastric cancer. Notably, various lncRNAs have been identified as promoters or inhibitors of tumorigenesis, and have been reported to be associated with drug resistance in gastric cancer (9,10). Yang *et al* (11) discovered that the expression levels of lncRNA urothelial cancer associated 1 were significantly upregulated in patients with gastric cancer based on analysis and validation of data from The Cancer Genome Atlas (TCGA) and the Genotype-Tissue Expression data project. Additionally, lncRNA urothelial cancer associated 1 was shown to be associated with increased cell proliferation and diminished apoptosis rates in gastric cancer cells (11). A previous study also highlighted the role of lncRNA maternally expressed gene 3 as a tumor suppressor in various types of cancer, including breast cancer, colorectal cancer and gastric cancer (12). Furthermore, lncRNAs are key signaling molecules that have been reported to be involved in the M2 macrophage polarization induced by gastric cancer cells. Xin *et al* (13) demonstrated that exosomes derived from gastric cancer can promote M2 macrophage polarization through lncRNA HCG2, thereby inducing gastric cancer metastasis. Additionally, Li *et al* (14) revealed that MKN4435 gastric cancer cells induced M2 macrophage polarization via exosome-mediated delivery of lncRNA MIR4435-2HG. All of these previous studies demonstrated that lncRNAs may serve an important role in the molecular networks of gastric cancer development. However, the regulatory mechanisms of lncRNAs in gastric cancer remain to be fully elucidated.

Previously, N6-methyladenosine (m6A) modification of lncRNAs has been recognized as a common mode of alteration that can induce changes in lncRNA functions (15). In gastric cancer, numerous m6A-related lncRNAs have been identified. Wang *et al* (16) identified 11 m6A-related lncRNAs, including AC010719.1 and AL049840.3, by examining TCGA gastric cancer-related data. Among these, six lncRNAs were considered to be potentially associated with the prognosis of patients with gastric cancer. Conversely, Zhang *et al* (17) proposed the reduced levels of m6A modification-induced mRNAs and lncRNAs in gastric cancer as a factor contributing to the malignant behaviors of cancer cells. These studies have suggested that m6A-modified lncRNAs may serve a key role in the development of gastric cancer; however, the precise functions and mechanisms of these lncRNAs require further exploration. Therefore, the present study aimed to analyze the key m6A-related lncRNAs significantly associated with the prognosis of patients with gastric cancer using existing high-throughput data linked to gastric cancer. Additionally, the functions and mechanisms of these lncRNAs were investigated through *in vitro* experiments.

Materials and methods

Data collection. TCGA database (https://cancergenome.nih.gov/) was used to download publicly available high-throughput sequencing data for gastric cancer-related lncRNAs, along with pathological information and follow-up data of patients with gastric cancer. The dataset included data from 446 tissue samples, consisting of 410 gastric cancer tissue samples and 36 adjacent non-tumorous tissue samples (Table SI). Additionally, 29 m6A feature target genes were obtained from the RM2Target platform (http://rm2target.canceromics.org/#/download).

Screening of m6A-related lncRNAs. To analyze m6A-related lncRNAs in gastric cancer tissues, Pearson correlation analysis was performed using the cor.test function in R version 4.4.0 (https://cran.r-project.org/). The analysis calculated Pearson correlation coefficients to determine the relationship between 29 m6A-related genes and lncRNAs in gastric cancer tissues. lncRNAs with a Pearson correlation coefficient >0.4 and P<0.05 were considered m6A-related lncRNAs. Subsequently, an interaction network diagram of m6A genes and related lncRNA genes was generated using Cytoscape version 3.9.1 (https://cytoscape.org/).

Screening of m6A-related differentially expressed lncRNAs (DElncRNAs) in gastric cancer. The DESeq2 R package (version 1.44.0; https://bioconductor.org/packages/release/bioc/html/DESeq2.html) was adopted for differential analysis of m6A-related lncRNA expression in gastric cancer and normal tissues. Briefly, m6A-related lncRNAs with |log2FoldChange|>2 and adjusted P-value (padj) <0.05 were considered m6A-related DElncRNAs. Volcano plots and heatmaps of m6A-related DElncRNAs were plotted using the ggplot2 (version 3.5.1; https://ggplot2.tidyverse.org) and pheatmap (version 1.0.12; https://github.com/raivokolde/pheatmap) packages, respectively.

Identification of prognosis-related m6A-modified lncRNAs in gastric cancer. Single-factor Cox regression analysis and multifactor Cox analysis were conducted on DElncRNAs using the survival (version 3.7-0; https://github.com/therneau/survival) and survminer (18) (version 0.4.9; https://rpkgs.datanovia.com/survminer.html) R packages. Single-factor Cox analysis was performed on m6A-related DElncRNAs and a forest plot was generated using the randomForest (version 4.7-1.2; https://www.stat.berkeley.edu/~breiman/RandomForests/) package. Subsequently, lasso regression analysis was carried out on m6A-related DElncRNAs at P<0.05 in single-factor Cox analysis using the glmnet (19) (version 4.1-8; https://glmnet.stanford.edu/) R package. A risk model was constructed based on the feature genes. The risk score was calculated using the following formula: RiskScore=$\Sigma\beta i$ x Gene, where βi represented the β-value corresponding to lncRNA, and Gene indicated the expression of the lncRNA. The median score was used as a threshold to divide patients into high-risk and low-risk groups. Survival differences between these groups were evaluated using Kaplan-Meier survival analysis and statistical significance was assessed using the log-rank test. Subsequently, the features identified in the lasso regression analysis were

incorporated into a multiple-factor Cox analysis, and a forest plot was generated.

Prediction of m6A sites in DElncRNAs. To further investigate the potential functional role of prognosis-related m6A-modified DElncRNAs in gastric cancer, the m6A modification sites were predicted within these DElncRNAs using the sequence-based RNA adenosine methylation site predictor tool (SRAMP; http://www.cuilab.cn/sramp). The SRAMP algorithm evaluated potential m6A-binding sites based on primary sequence motifs and structural features, providing confidence scores categorized as very high, moderate or low confidence.

Cell culture. Normal gastric epithelial cells (GES-1), human gastric cancer cells (AGS and MKN-45) and human monocytes (THP-1) were used in the present study. All cell lines were obtained from the American Type Culture Collection. GES-1, MKN-45 and THP-1 cells were cultured in Roswell Park Memorial Institute (RPMI)-1640 medium supplemented with 10% fetal bovine serum (FBS) and 1% penicillin-streptomycin (all from Gibco; Thermo Fisher Scientific, Inc.), whereas AGS cells were cultured in Dulbecco's Modified Eagle Medium/F12 (DMEM/F12; Gibco; Thermo Fisher Scientific, Inc.) supplemented with 10% FBS and 1% penicillin-streptomycin. All cells were maintained at 37˚C with 5% CO_2.

Cell transfection. AGS and MKN-45 cells were transfected with short hairpin (sh)RNA constructs targeting YT521-B homology domain family member 2 (YTHDF2; sh-YTHDF2), AC026691.1 (sh-AC026691.1) or a non-targeting control (sh-NC), which had been inserted into the pSUPER vector backbone (OligoEngine), using the Neofect™ DNA transfection reagent [cat. no. TF201201; Neofect (Beijing) Biotech Co., Ltd.]. For co-transfection experiments, sh-YTHDF2 and sh-AC026691.1 plasmids were mixed in equal amounts. Transfections were performed according to the manufacturer's protocol. Briefly, 2 μg plasmid DNA was used per well in a 6-well plate. The plasmid DNA was diluted in serum-free RPMI-1640 medium or DMEM/F12 and incubated with Neofect DNA Transfection Reagent at room temperature for 20 min to form transfection complexes. AGS and MKN-45 cells were seeded at a density of $1x10^5$ cells/well and were allowed to reach ~70% confluence prior to transfection. The transfection complexes were added dropwise to the culture wells and incubated with the cells at 37˚C in a humidified atmosphere containing 5% CO_2 for 48 h. Immediately after the incubation, the supernatant was collected, centrifuged at 200 x g for 10 min at 4˚C to remove debris, and stored for subsequent experiments. Successfully transfected cells were used to assess the effects of shRNA-mediated knockdown on target gene expression and function. The shRNA sequences were designed and synthesized by Shanghai GeneChem Co., Ltd., as follows: sh-YTHDF2: 5'-GGAAATCCAGAGGAG CCAATA-3'; sh-AC026691.1: 5'-GCTGAGGTCTTCCTA GATAAT-3'; sh-NC: 5'-TTCTCCGAACGTGTCACGT-3'.

THP-1 differentiation and co-culture. THP-1 cells were incubated with phorbol 12-myristate 13-acetate (cat. no. 16561-29-8; MedChemExpress) for 24 h to induce their differentiation into M0 macrophages (20). Subsequently, M0 macrophages were cultured with 2 ml cell supernatants collected from AGS and MKN-45 cells transfected with sh-NC, sh-YTHDF2 or sh-AC026691.1, or co-transfected with sh-AC026691.1 and sh-YTHDF2. Macrophages were divided into four groups corresponding to the experimental conditions and incubated at 37˚C with 5% CO_2 for 48 h for further analysis.

Reverse transcription quantitative polymerase chain reaction (RT-qPCR). Total RNA was extracted from cells in each group using TRNzol Universal Reagent (cat. no. DP424; Tiangen Biotech Co., Ltd.). Subsequently, 1,000 ng extracted RNA was reverse transcribed into cDNA using the lnRcute lncRNA First-Strand cDNA Kit (cat. no. KR202; Tiangen Biotech Co., Ltd.) and FastKing cDNA First-Strand Synthesis Kit (cat. no. KR116; Tiangen Biotech Co., Ltd.) according to the manufacturer's instructions, prior to qPCR. Subsequently, the Talent qPCR PreMix (SYBR Green) (cat. no. FP209; Tiangen Biotech Co., Ltd.) was used to perform qPCR on the LightCycler 480 Real-Time Fluorescent Quantitative PCR System (Roche Diagnostics). The thermal cycling procedures were as follows: 95˚C for 3 min, followed by 40 cycles at 95˚C for 5 sec and 60˚C for 15 sec. The melt curve data were collected to verify the specificity of PCR and to confirm the absence of primer dimers. GAPDH served as an endogenous control gene for normalization of target gene expression using the $2^{-\Delta\Delta Cq}$ method (20). All primers were synthesized by Sangon Biotech Co., Ltd. and are listed in Table I. Each experiment was conducted at least three times.

Methylated RNA immunoprecipitation-qPCR (MeRIP-qPCR). The extracted RNA was fragmented using the Q800R3 DNA Shearing Sonicator at 20 kHz for 5 min at 4˚C (Qsonica LLC). Subsequently, m6A antibody (1:50; cat. no. ab151230; Abcam) was diluted to 1 μg/μl and added to the fragmented RNA (1 μg) for 4 h at 4˚C. Following incubation, 50 μl Pierce Protein A/G Magnetic Beads (cat. no. 10002D; Thermo Fisher Scientific, Inc.) were then added and incubated for another 1 h at 4˚C. The magnetic beads were immobilized using a magnetic rack and the supernatant was removed. Subsequently, the beads were rinsed with 200 μl wash buffer (PBS containing 0.05% Tween-20), gently mixed with the m6A antibody-bound RNA complexes and incubated at 4˚C for 5 min. Then, the beads were immobilized using the magnetic rack and the supernatant was removed. This step was performed twice. Subsequently, the RNA was extracted from the beads and reverse transcribed. Finally, RT-qPCR was performed according to the aforementioned protocol to detect the expression levels of AC026691.1. Each enrichment experiment was repeated three times.

RNA pull-down assay. Cells cultured under normal conditions were collected into 1.5-ml Eppendorf tubes. Next, the cells were supplemented with RNA binding buffer (cat. no. 65042D; Thermo Fisher Scientific, Inc.) containing protease inhibitors (cat. no. 78429; Thermo Fisher Scientific, Inc.), ribonuclease inhibitors (cat. no. 10777019; Thermo Fisher Scientific, Inc.) and dithiothreitol (cat. no. R0861; Thermo Fisher Scientific, Inc.), and completely fragmented using a Qsonica Q800R3 DNA Shearing Sonicator at 20 kHz for 5 min at 4˚C. Upon removal of cell debris, 2 μg biotin-labeled probes, including AC026691.1 (target probe) and the negative control (NC)

Table I. Quantitative PCR primers.

Gene	Sequence, 5'-3'
AC026691.1	F: CTCACCGGGATGCTTTACACC
	R: ATCCAGCACCCAAATCGATG
YTHDF2	F: TAGCCAGCTACAAGCACACCAC
	R: CAACCGTTGCTGCAGTCTGTGT
iNOS	F: GCTCTACACCTCCAATGTGACC
	R: CTGCCGAGATTTGAGCCTCATG
IL-6	F: AGACAGCCACTCACCTCTTCAG
	R: TTCTGCCAGTGCCTCTTTGCTG
Arg-1	F: TCATCTGGGTGGATGCTCACAC
	R: GAGAATCCTGGCACATCGGGAA
IL-10	F: TCTCCGAGATGCCTTCAGCAGA
	R: TCAGACAAGGCTTGGCAACCCA
GAPDH	F: CATCACTGCCACCCAGAAGACTG
	R: ATGCCAGTGAGCTTCCCGTTCAG

F, forward; R, reverse; YTHDF2, YT521-B homology domain family member 2; iNOS, inducible nitric oxide synthase; Arg-1, arginase 1.

probe (custom-synthesized by Sangon Biotech Co., Ltd.), were added to the cell lysate. The mixture was then incubated at 30˚C for 30 min to form RNA-protein complexes. After incubation, the complexes were incubated with streptavidin agarose at room temperature for 50 min. To ensure the specificity of the RNA-protein interactions, IgG control (1:1,000; cat. no. ab172730; Abcam) was added at this stage of the experiment. Subsequently, the complexes were washed five times with 1X SDS-PAGE loading buffer (Beyotime Institute of Biotechnology). Finally, the protein was extracted for western blot analysis. Each pull-down assay was performed in triplicate.

RNA stability analysis. Post-transfection with different shRNA vectors, the cells were treated with 10 μg/ml actinomycin D (Sigma-Aldrich; Merck KGaA) at 37˚C for various durations (0, 4, 8 and 12 h). Total RNA from each cell group was extracted using TRNzol Universal Reagent at the specified time points (0, 4, 8 and 12 h), and RT-qPCR was performed according to the aforementioned protocol to measure the mRNA expression levels of AC026691.1. RNA stability experiments were repeated three times.

MTT assay. Cells (~2x10^4 cells/well) were seeded in a 96-well cell plate and MTT (cat. no. 298-93-1; MedChemExpress) was added to each well upon 24 h of culture. After 4 h of incubation at 37˚C with MTT, the supernatant was removed, followed by the addition of 150 μl dimethyl sulfoxide to dissolve the formazan crystals. Subsequently, absorbance was assessed at an optical density of 562 nm using the SpectraMax ABS Plus (Molecular Devices, LLC) to detect cell viability.

Colony formation assay. Cell proliferation was determined using the colony formation assay. Specifically, cells (4x10^2 cells/well) were seeded into a 6-well plate. Post-transfection, cells were cultured for 14 days or until the majority of single clones contained >50 cells. Subsequently, the cells were fixed with 4% paraformaldehyde at room temperature for 30 min, and stained with 0.1% crystal violet at room temperature for 15 min. Images were captured and the number of colonies formed was counted manually. Each experiment was conducted in triplicate.

Transwell assay. A Transwell assay was used to assess cell migration. Briefly, 2x10^4 transfected cells were seeded into the upper chamber of 24-well Transwell assay inserts (pore size, 8 μm; cat. no. 3422; Corning, Inc.). The upper chamber was supplemented with serum-free RPMI-1640 medium or DMEM/F12, while the lower chamber was supplemented with RPMI-1640 medium or DMEM/F12 containing 20% FBS. The cells were then incubated at 37˚C with 5% CO_2 for 20-24 h. Subsequently, the cells in the upper chamber were carefully removed with a cotton swab. The cells that had migrated to the lower surface were fixed with 4% paraformaldehyde at room temperature for 15 min, stained with 0.1% crystal violet at room temperature for 30 min, washed with phosphate-buffered saline and air-dried. The migrated cells were counted under a light microscope (CX23; Olympus Corporation). Each experiment was conducted in triplicate.

Flow cytometry. The impact of AC026691.1 expression in AGS and MKN-45 gastric cancer cells on the polarization of M0 macrophages (derived from THP-1 cells) was assessed using Alexa Fluor® 647-conjugated rabbit recombinant monoclonal CD80 antibody (1:500, cat. no. ab307467; Abcam) and fluorescein isothiocyanate-conjugated mouse monoclonal CD206 antibody (1:25, cat. no. ab270647; Abcam). Approximately 1x10^6 cells from each group were collected and incubated with the antibodies in the dark for 1 h at 4˚C. The expression of CD80 and CD206 was observed using a flow cytometer (NovoCyte Advanteon; Agilent Technologies, Inc.), and the resulting data were analyzed using FlowJo 7.6 software (FlowJo; BD Biosciences). The excitation and emission wavelengths for the CD80 antibody were 647 and 668 nm, respectively; and for the CD206 antibody, they were 495 and 528 nm, respectively. Each experiment was conducted in triplicate.

Western blot analysis. Cells were lysed in RIPA lysis buffer containing phenylmethylsulfonyl fluoride protease inhibitor (Wuhan Boster Biological Technology, Ltd.) and disrupted using a Qsonica Q800R3 DNA Shearing Sonicator at 20 kHz for 5 min at 4˚C. The concentration of extracted protein was determined using a bicinchoninic acid protein quantification kit (Beijing Solarbio Science & Technology Co., Ltd.). Subsequently, proteins (20 μg) were separated by SDS-PAGE on a 12% polyacrylamide gel and transferred onto a 0.45-μm polyvinylidene fluoride membrane (Bio-Rad Laboratories, Inc.). The membrane was then blocked with 5% skimmed milk for 3 h at room temperature and incubated with primary antibodies overnight at 4˚C. The following primary antibodies were used: YTHDF2 (1:1,000; cat. no. ab220163), E-cadherin (1:1,000; cat. no. ab314063), N-cadherin (1:1,000; cat. no. ab76011), matrix metalloproteinase-9 (MMP-9; 1:1,000; cat. no. ab76003) and GAPDH (1:1,000; cat. no. ab8245) (all from Abcam). The following day, the membrane was incubated

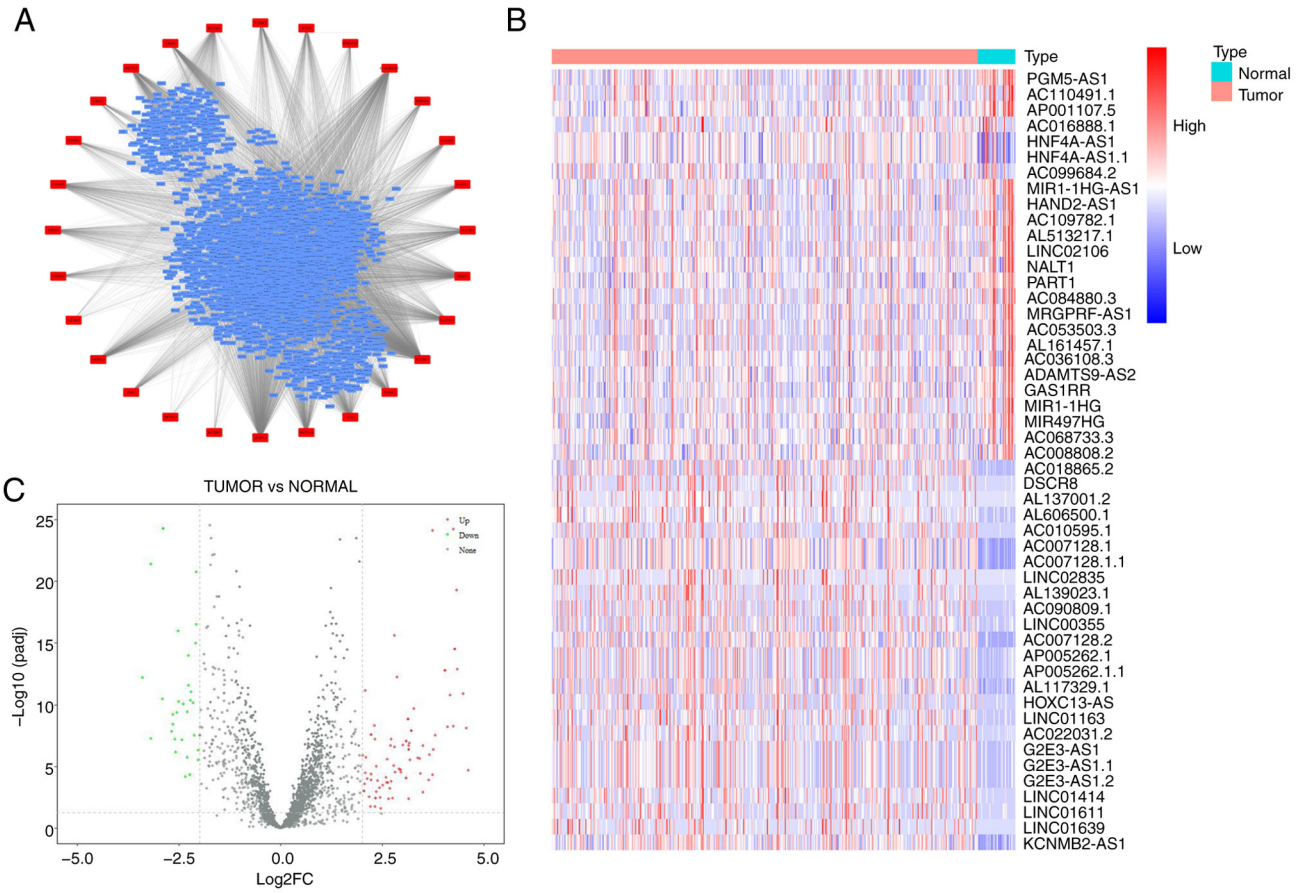

Figure 1. Identification of m6A-related DElncRNAs in gastric cancer. (A) Network diagram illustrating the correlation between m6A-related genes and lncRNAs in gastric cancer. The red modules represent m6A-related genes and the blue modules indicate lncRNAs. (B) Heatmap (top 50) and (C) volcano plot displaying the expression of m6A-related DElncRNAs in gastric cancer tissues and normal tissues. m6A, N6-methyladenosine; lncRNAs, long non-coding RNAs; DElncRNAs, differentially expressed lncRNAs; FC, fold change.

with horseradish peroxidase-conjugated anti-rabbit secondary antibody (1:5,000; cat. no. ab205718; Abcam) or anti-mouse secondary antibody (1:5,000; cat. no. ab205719; Abcam) at room temperature for 2 h. Subsequently, enhanced chemiluminescent luminescence reagent (cat. no. C510043; Sangon Biotech Co., Ltd.) was used for detection. Protein bands were visualized using a chemiluminescence imaging system (Amersham; Cytiva). Finally, the intensity of protein bands was semi-quantified using ImageJ version 1.53 (National Institutes of Health). Each western blot analysis was conducted in triplicate.

Statistical analysis. Statistical analysis was conducted using GraphPad Prism 8.0 software (Dotmatics). Differences between groups were compared using unpaired Student's t-test, whereas a one-way analysis of variance followed by Tukey's post hoc test was used to compare the differences among three or more groups. Data are presented as the mean ± standard deviation from at least three independent experiments. P<0.05 was considered to indicate a statistically significant difference.

Results

Identification of m6A-related DElncRNAs in gastric cancer. To identify m6A-related lncRNAs associated with gastric cancer prognosis, gastric cancer lncRNA expression datasets were obtained from TCGA database and 29 m6A-related genes from RM2Target were used to conduct a correlation analysis. A total of 8,003 lncRNAs were identified to be significantly correlated with 28 m6A-related genes based on the screening criteria of correlation coefficient >0.4 and P<0.05 (Fig. 1A). Subsequently, a differential expression analysis was performed on the 8,003 lncRNAs in gastric cancer, and a total of 126 m6A-related DElncRNAs were screened, including 95 upregulated and 31 downregulated lncRNAs, according to the criteria of |log2FoldChange|>2 and padj <0.05 (Fig. 1B and C).

Identification of prognostic m6A-related DElncRNAs in gastric cancer. To further elucidate prognostic m6A-related DElncRNAs in gastric cancer, a single-factor Cox regression analysis was performed on the 126 m6A-related DElncRNAs. The analysis results revealed that 29 m6A-related DElncRNAs were significantly associated with the prognosis of patients with gastric cancer, all with hazard ratios of <1 (Fig. 2A). Such results indicated that these lncRNAs were protective factors in gastric cancer. The statistical significance was assessed using a P-value threshold of <0.05.

Furthermore, the R package glmnet was used to conduct a lasso regression analysis on the 29 m6A-related DElncRNAs, identifying nine feature variables: AC026691.1, AC084880.3, AC090809.1, AC107308.1, AC109782.1, AP005262.1, GAS1RR, LINC02106 and MRGPRF-AS1

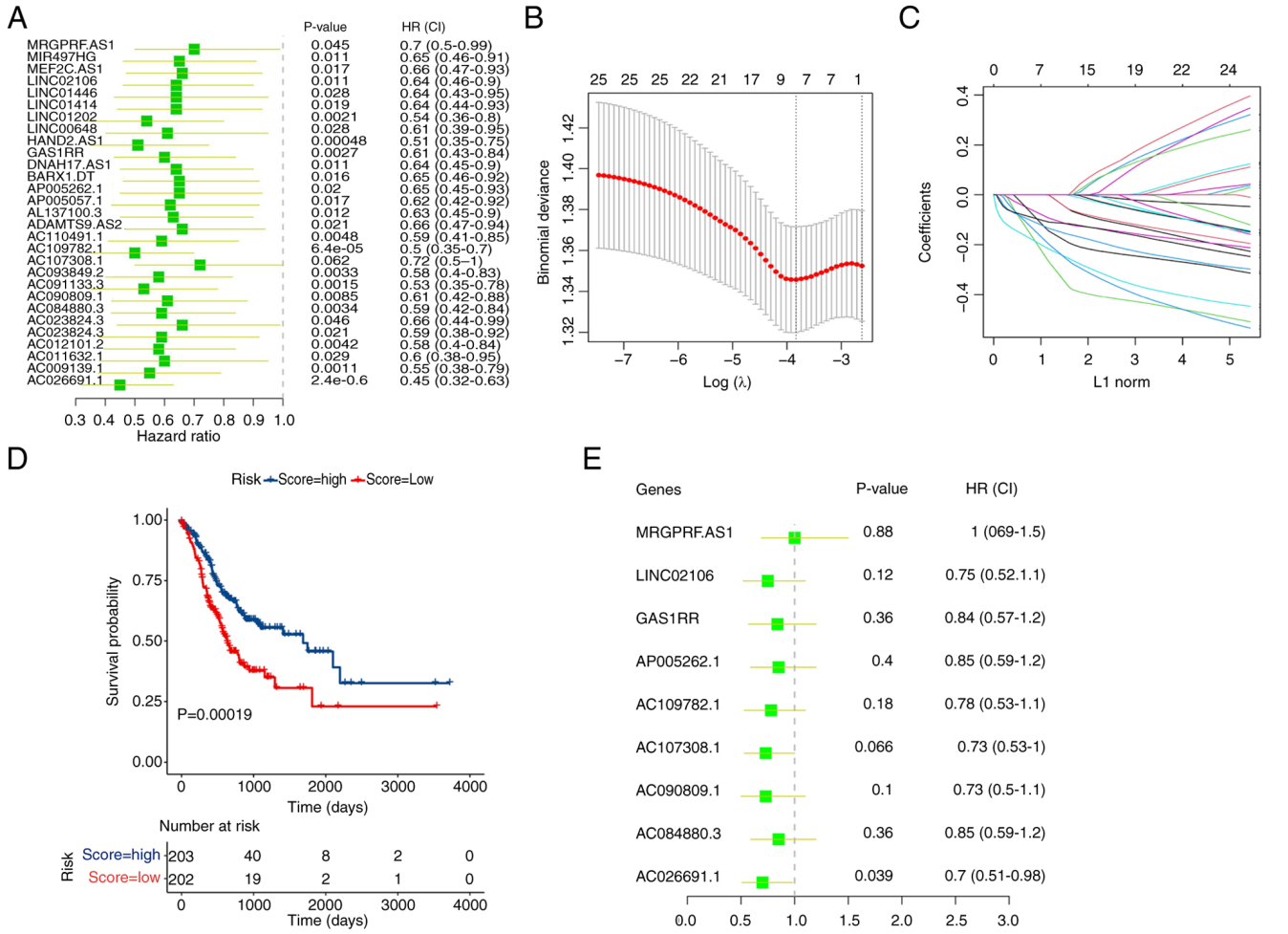

Figure 2. Identification of prognostic m6A-related DElncRNAs in gastric cancer. (A) Forest plot displaying the results of single-factor Cox regression analysis for 29 m6A-related DElncRNAs. (B) Determination of the optimal penalization coefficient λ in the lasso regression model using 10-fold cross-validation and minimum criteria. The shaded area represents the 95% CI for the λ selection. (C) Lasso coefficient profiles of the m6A-related DElncRNAs. (D) Kaplan-Meier survival curves stratifying patients with gastric cancer into the high-risk and low-risk groups based on the median risk score calculated from the lasso regression model. (E) Forest plot illustrating the outcomes of single-factor Cox regression analysis for nine m6A-related DElncRNAs. m6A, N6-methyladenosine; DElncRNAs, differentially expressed long non-coding RNAs, HR, hazard ratio; CI, confidence interval.

(Fig. 2B and C). The optimal λ value was selected based on cross-validation to minimize the mean cross-validated error. Risk scores were calculated using the following formula: Risk score=(-0.013 x AC026691.1) + (-0.099 x AC084880.3) + (-0.155 x AC090809.1) + (-0.288 x AC107308.1) + (-0.139 x AC109782.1) + (-0.0135 x AP005262.1) + (-0.225 x GAS1RR) + (-0.212 x LINC02106) + (-0.111 x MRGPRF-AS1).

The Kaplan-Meier method was adopted for survival analysis based on the median risk score, and the difference in survival between the high-risk and low-risk groups was assessed using the log-rank test. The results revealed that patients with a higher risk score had a significantly better survival rate compared to those with a lower risk score (P=0.00019; Fig. 2D). To further validate the prognostic value of the identified lncRNAs, a multivariate Cox analysis was conducted on the nine feature variables. This analysis demonstrated that AC026691.1 (hazard ratio=0.7, P=0.039) was notably associated with the prognosis of patients with gastric cancer (Fig. 2E). The proportional hazards assumption was tested and satisfied, ensuring the validity of the Cox model.

These detailed analyses indicated the protective role of certain m6A-related lncRNAs in gastric cancer and highlighted AC026691.1 as a significant prognostic factor.

Downregulation of lncRNA AC026691.1 in gastric cancer cells. Bioinformatics analysis identified m6A-related DElncRNAs associated with gastric cancer prognosis, including AC026691.1. Subsequently, the expression levels of lncRNA AC026691.1 were examined in normal gastric epithelial cells (GES-1) and human gastric cancer cells (AGS and MKN-45). The results revealed a marked downregulation in the expression levels of AC026691.1 in AGS and MKN-45 cells compared with those in GES-1 cells (P<0.01; Fig. 3).

YTHDF2 promotes m6A modification-mediated degradation of AC026691.1 in gastric cancer cells. To investigate the role of m6A modification in AC026691.1, potential m6A sites were predicted using the SRAMP tool. The results exhibited three potential m6A-binding sites between lncRNA AC026691.1 and YTHDF2, located at positions 1,103 (very high confidence), 1,121 (moderate confidence) and 2,042 (low confidence)

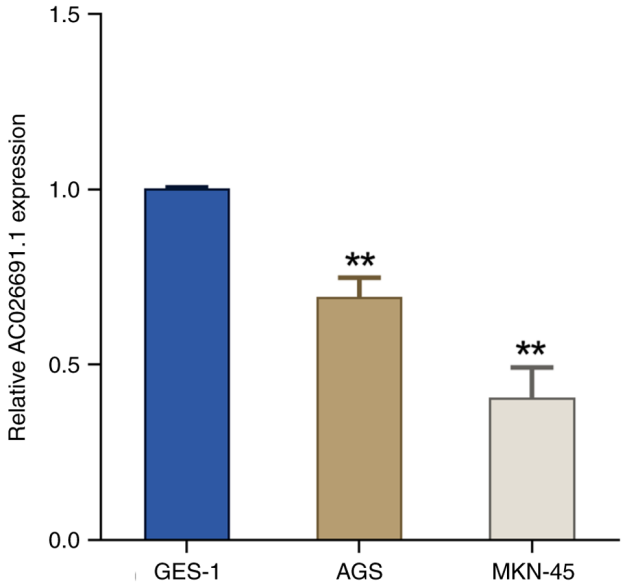

Figure 3. Downregulation of lncRNA AC026691.1 in gastric cancer cells. Reverse transcription-quantitative polymerase chain reaction analysis of the expression levels of lncRNA AC026691.1 in normal gastric epithelial cells (GES-1) and human gastric cancer cells (AGS and MKN-45), **P<0.01 vs. GES-1. lncRNA, long non-coding RNA.

(Fig. 4A). The MeRIP-qPCR experiments confirmed that m6A modification was enriched in lncRNA AC026691.1, and the expression levels of m6A-modified AC026691.1 were markedly higher in gastric cancer cells AGS and MKN-45 than those in GES-1 cells (P<0.01; Fig. 4B). Additionally, the expression of YTHDF2 was notably upregulated in AGS and MKN-45 cells as opposed to in GES-1 cells (Fig. 4C).

Subsequently, the expression of YTHDF2 was knocked down in AGS and MKN-45 cells to validate the hypothesis that YTHDF2 may mediate the degradation of m6A-modified AC026691.1. The results of RT-qPCR and western blot analysis showed that the expression levels of AC026691.1 were markedly increased in the sh-YTHDF2 group compared with those in the sh-NC group, while the expression of YTHDF2 was downregulated (Fig. 4D-G). The results of RNA pull-down assays confirmed the interaction between AC026691.1 and YTHDF2 (Fig. 4H). Furthermore, RNA stability analysis indicated that AC026691.1 stability was significantly higher in the sh-YTHDF2 group than that in the sh-NC group (Fig. 4I). These results suggested that YTHDF2 may promote the degradation of m6A-modified AC026691.1 in gastric cancer cells.

YTHDF2 knockdown inhibits gastric cancer cell proliferation and migration by reducing m6A-modified AC026691.1. Given the role of m6A-related lncRNA in gastric cancer, it was hypothesized that m6A-modified AC026691.1 might contribute to gastric cancer progression. To test this hypothesis, YTHDF2 and AC026691.1 were knocked down individually or simultaneously in AGS and MKN-45 cells. The results of RT-qPCR demonstrated that in contrast to the sh-NC group, the expression levels of AC026691.1 were increased in the sh-YTHDF2 group, whereas they were decreased in the sh-AC026691.1 group. Additionally, the sh-AC026691.1 + sh-YTHDF2 group exhibited intermediate levels of AC026691.1 (P<0.01; Fig. 5A).

Subsequently, the effects of YTHDF2 and/or AC026691.1 knockdown on gastric cancer cell viability, colony formation and migration were assessed. Knockdown of YTHDF2 significantly reduced cell viability, colony formation and migration, while knockdown of AC026691.1 exhibited the opposite effect; whereas simultaneous knockdown of both genes reversed the respective effects (P<0.01; Fig. 5B-D). Additionally, knockdown of YTHDF2 resulted in a notable upregulation in E-cadherin, and a downregulation in N-cadherin and MMP-9 in gastric cancer cells; however, knockdown of AC026691.1 had the opposite effects. The double knockdown restored the expression of E-cadherin, N-cadherin and MMP-9 to near-control levels, reversing the effects observed in the single knockdown groups (P<0.01; Fig. 5E-H). These findings suggested that YTHDF2 inhibited gastric cancer cell proliferation, migration and epithelial-mesenchymal transition (EMT) by promoting the degradation of m6A-modified AC026691.1, thereby reducing its oncogenic potential.

YTHDF2 knockdown suppresses M2 macrophage polarization by reducing m6A modification of AC026691.1. Macrophage polarization in the tumor microenvironment is closely related to gastric cancer cell metastasis and EMT processes (21). To explore whether m6A modification of AC026691.1 affects macrophage polarization, YTHDF2 and/or AC026691.1 were knocked down in AGS and MKN-45 cells, and macrophages were incubated with conditioned medium. Compared with in the sh-NC group, sh-YTHDF2 increased the expression levels of inducible nitric oxide synthase (iNOS) and IL-6, and decreased the expression levels of arginase-1 (Arg-1) and IL-10 in macrophages; however, sh-AC026691.1 exhibited the opposite effects. Furthermore, intermediate levels of these genes were observed in the sh-AC026691.1 + sh-YTHDF2 group (P<0.01; Fig. 6A). Flow cytometric analysis further confirmed these findings, showing a significant elevation in the proportion of CD80-positive macrophages and a decrease in CD206-positive macrophages in the sh-YTHDF2 group; however, opposite trends were detected in the sh-AC026691.1 group, and the double knockdown group exhibited intermediate effects (P<0.01; Fig. 6B). These findings demonstrated the role of YTHDF2 in mediating AC026691.1-induced M2 macrophage polarization. Overall, these results indicated that knockdown of YTHDF2 reduced M2 macrophage polarization through promoting the degradation of m6A-modified AC026691.1, highlighting a novel regulatory mechanism in the tumor microenvironment.

Discussion

Patients with gastric cancer face various challenges, including poor treatment outcomes and prognosis, which are primarily caused by an unclear understanding of the mechanisms underlying gastric cancer development (22). Recent studies have highlighted the key role of m6A-related lncRNAs in the process of cancer development, including gastric cancer (23) and colorectal cancer (24). However, m6A-related lncRNAs with pivotal roles in gastric cancer development have yet to be discovered due to the diversity of lncRNAs and the complexity of the m6A modification. In the present study,

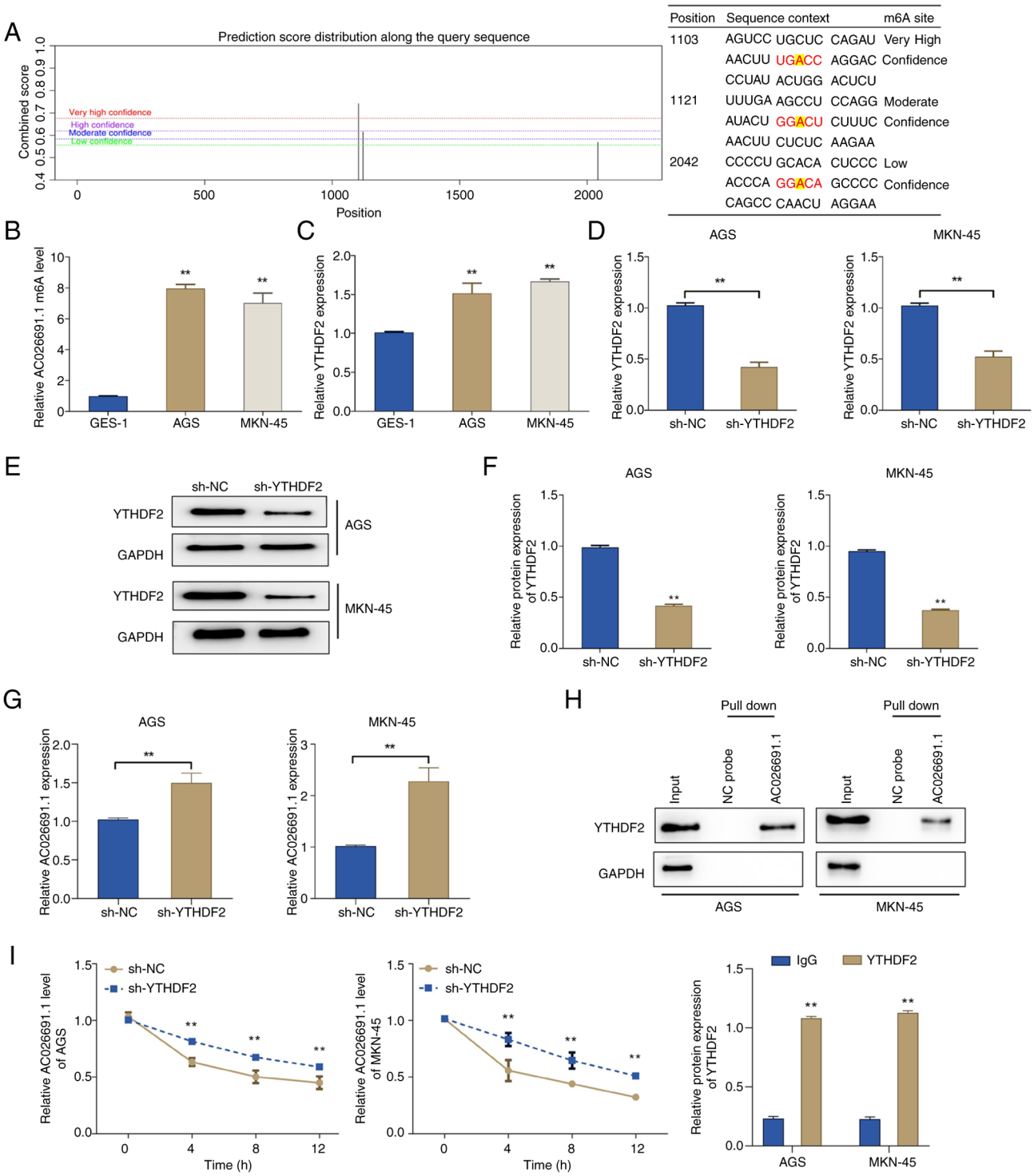

Figure 4. YTHDF2 promotes the degradation of m6A-modified AC026691.1 in gastric cancer cells. (A) Potential m6A modification sites in the AC026691.1 sequence predicted by sequence-based RNA adenosine methylation site predictor. (B) Methylated RNA immunoprecipitation qPCR assay was performed to determine the m6A modification levels of AC026691.1 in GES-1, AGS and MKN-45 cells. (C) RT-qPCR analysis of YTHDF2 expression levels in different cell types. **P<0.01 vs. GES-1. (D) RT-qPCR analysis and (E) western blot analysis of YTHDF2 expression in gastric cancer cells transfected with sh-NC and sh-YTHDF2. (F) Semi-quantification of YTHDF2 protein expression in gastric cancer cells transfected with sh-NC and sh-YTHDF2. (G) RT-qPCR to examine the expression levels of AC026691.1 in gastric cancer cells following YTHDF2 knockdown. **P<0.01 vs. sh-NC. (H) RNA pull-down assay to observe the interaction between AC026691.1 and YTHDF2. **P<0.01, vs. IgG. (I) Actinomycin D was used to observe the stability of AC026691.1 in cells after YTHDF2 knockdown. **P<0.01 vs. sh-NC. YTHDF2, YT521-B homology domain family member 2; m6A, N6-methyladenosine; RT-qPCR, reverse transcription qPCR; qPCR, quantitative polymerase chain reaction; sh, short hairpin; NC, negative control.

TCGA and bioinformatics methods were employed to identify key m6A-related DElncRNAs significantly associated with the prognosis of patients with gastric cancer.

Epitranscriptomics has been found to serve a crucial role in various cellular functions and has garnered increasing attention (1,25). Currently, >100 types of chemical modifications

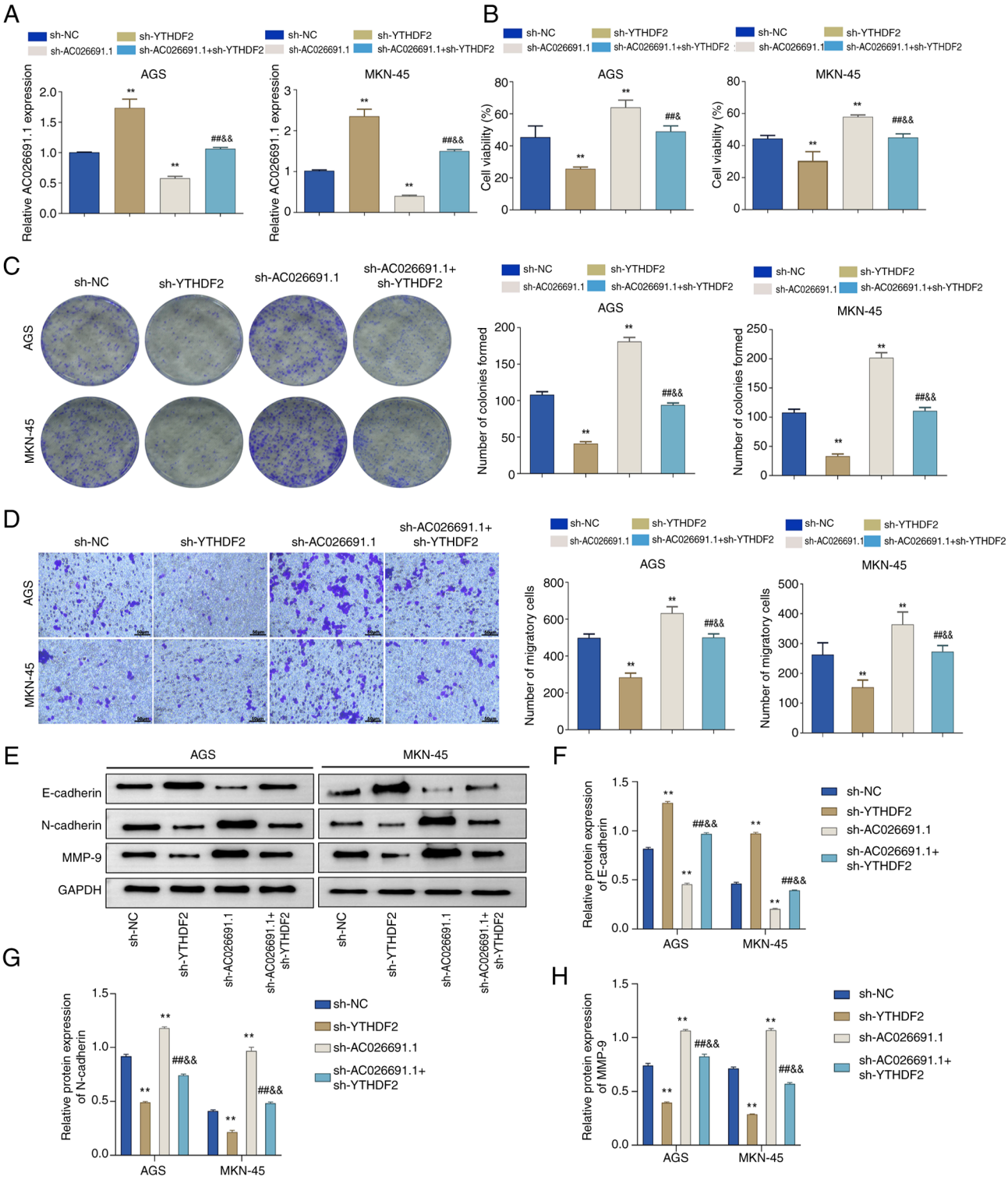

Figure 5. YTHDF2 knockdown suppresses gastric cancer cell proliferation and migration by reducing m6A modification of AC026691.1. (A) Reverse transcription-quantitative polymerase chain reaction analysis of AC026691.1 expression levels in AGS and MKN-45 cells following YTHDF2 and/or AC026691.1 knockdown. (B) MTT, (C) colony formation and (D) Transwell assays (scale bar: 50 μM) were performed to assess the viability, colony formation and migration of AGS and MKN-45 cells after YTHDF2 and/or AC026691.1 knockdown. (E) Representative Western blot images showing the protein levels of E-cadherin, N-cadherin and MMP-9 in AGS and MKN-45 cells following YTHDF2 and/or AC026691.1 knockdown. Semi-quantification of relative protein expression of (F) E-cadherin, (G) N-cadherin and (H) MMP-9. **P<0.01 vs. sh-NC; $^{\#\#}$P<0.01 vs. sh-YTHDF2; $^{\&\&}$P<0.01 vs. sh-AC026691.1. YTHDF2, YT521-B homology domain family member 2; MMP-9, matrix metalloproteinase-9; sh, short hairpin; NC, negative control.

have been discovered in various RNAs (26). Among these, m6A methylation is a well-studied intracellular transcription modification occurring in eukaryotic mRNA, microRNA, lncRNA and circular RNA (27-30). m6A is an epigenetic modification of RNA controlled by three types of enzymes, mainly mediated by m6A methyltransferases (writers), m6A modification site recognition proteins (readers) and demethylases (erasers) (31). Specifically, the writers are responsible

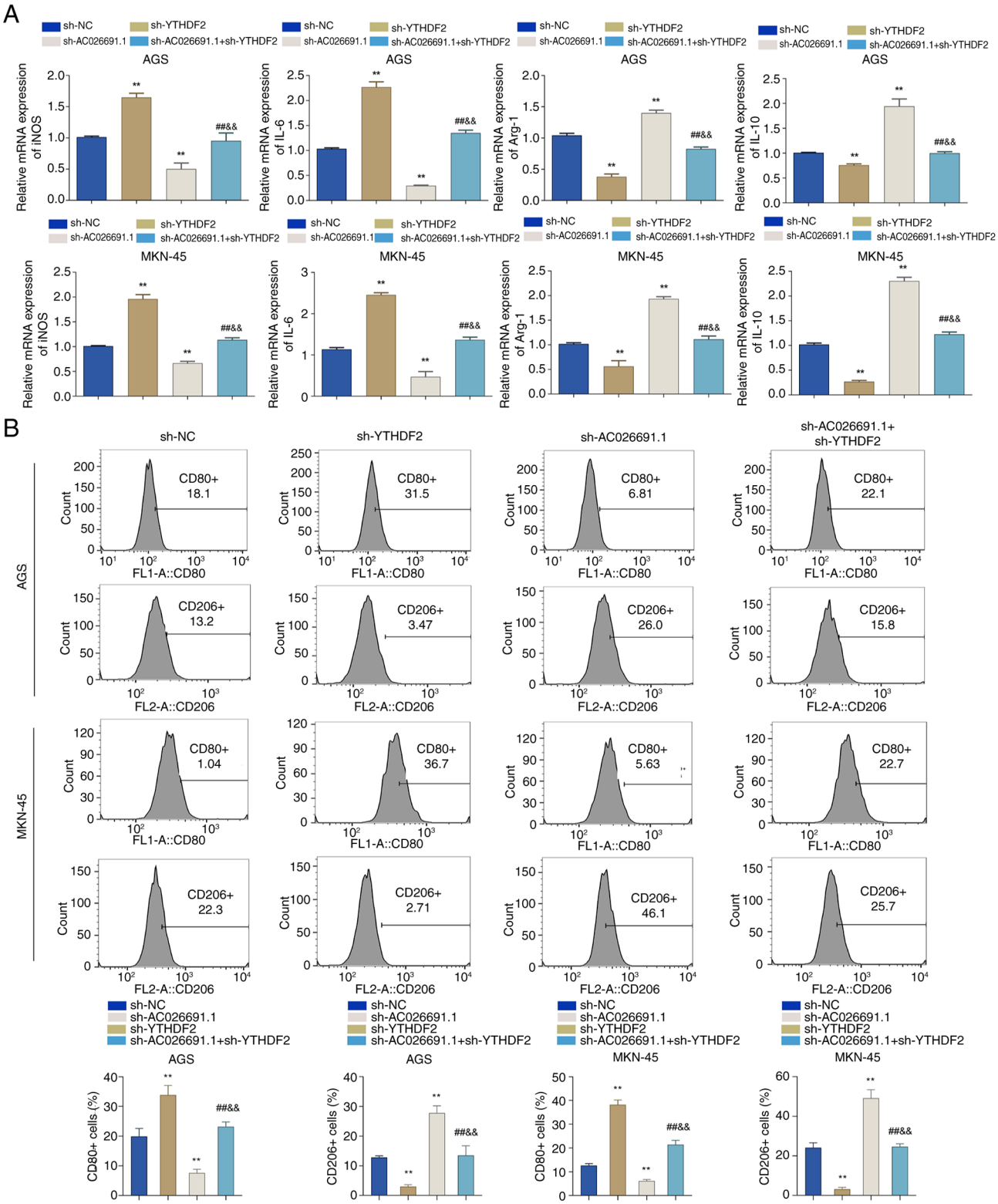

Figure 6. YTHDF2 knockdown suppresses M2 macrophage polarization by reducing m6A modification of AC026691.1. (A) Reverse transcription-quantitative polymerase chain reaction analysis of iNOS, IL-6, Arg-1 and IL-10 expression levels in macrophages co-cultured with conditioned medium from AGS and MKN-45 cells following YTHDF2 and/or AC026691.1 knockdown. (B) Flow cytometry was performed to assess CD80- and CD206-positive macrophages in conditioned medium co-cultured with AGS and MKN-45 cells following YTHDF2 and/or AC026691.1 knockdown. **P<0.01 vs. sh-NC; $^{\#\#}$P<0.01 vs. sh-YTHDF2; $^{\&\&}$P<0.01 vs. sh-AC026691.1. iNOS, inducible nitric oxide synthase; Arg-1, arginase-1; YTHDF2, YT521-B homology domain family member 2; sh, short hairpin; NC, negative control.

for adding methyl groups to the specific nucleotides, readers recognize modified adenine or cytosine to exert specific functions, and erasers remove methyl marks (32). In the present study, m6A-related lncRNAs were screened based on their correlation with m6A-related genes. Subsequently, differential expression, Cox regression and lasso regression analyses

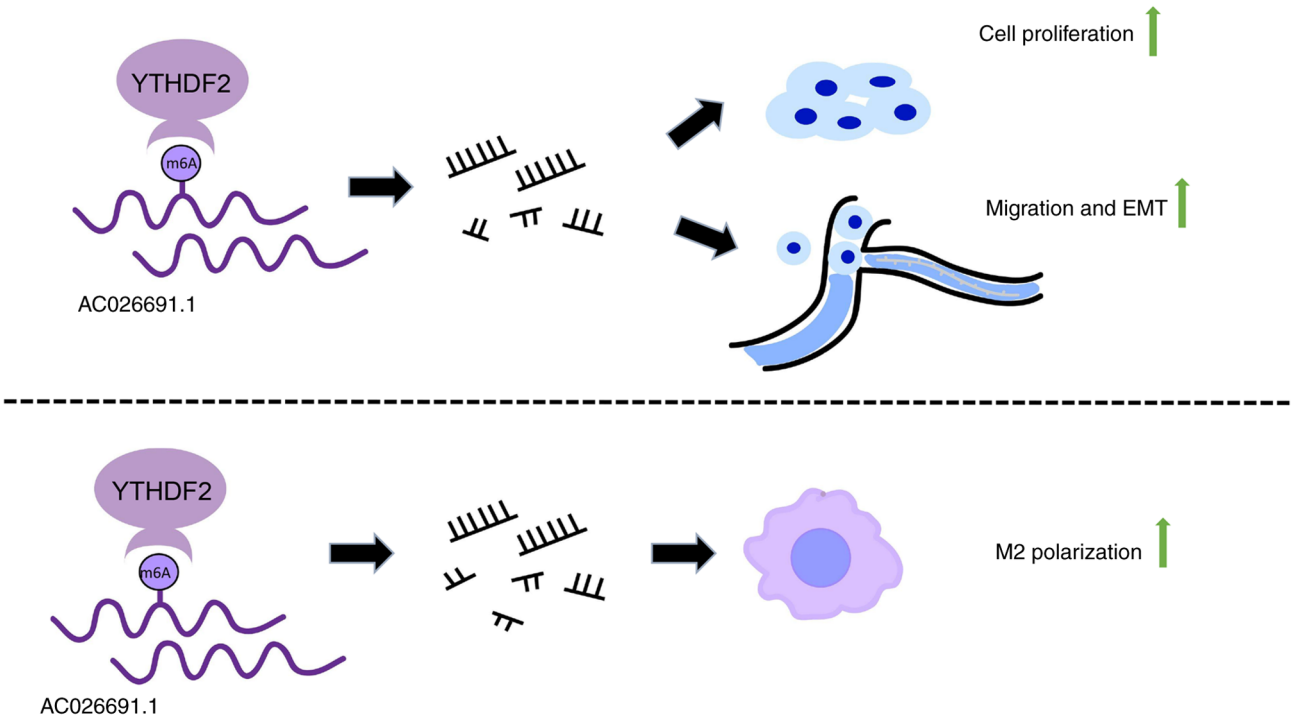

Figure 7. Mechanism of YTHDF2-induced degradation of AC026691.1 to promote gastric cancer progression. EMT, epithelial-mesenchymal transition; m6A, N6-methyladenosine; YTHDF2, YT521-B homology domain family member 2.

were utilized to identify m6A-related DElncRNAs (such as AC026691.1) associated with the prognosis of patients with gastric cancer.

AC026691.1 has previously been shown to be linked to m6A modification and to exhibit a notable downregulation in the tumor tissues of patients with gastric cancer (33). Although the low expression of AC026691.1 has been demonstrated to increase the proliferation and migration of gastric cancer cells, its specific functions and underlying mechanisms remain to be explored (33). In the present study, the expression levels of AC026691.1 were significantly decreased in gastric cancer cells, which is consistent with previous studies (33,34). Sequence-based RNA adenosine methylation site predictor was subsequently used, and the results suggested that m6A-modified AC026691.1 may interact with YTHDF2. Such a relationship was confirmed by methylated RNA immunoprecipitation qPCR and RNA pull-down experiments. YTHDF2, a member of the YTH domain protein family, primarily functions as a m6A reader that recognizes m6A modifications and accelerates the degradation of m6A-modified RNA (35), including lncRNA (36). In the present study, an obvious decrease was observed in the expression and stability of AC026691.1 in gastric cancer cells following YTHDF2 knockdown, suggesting that YTHDF2 could recognize and facilitate the degradation of m6A-modified AC026691.1.

Although research on AC026691.1 is limited, the effect of YTHDF2 on cancer has been extensively studied. Fang *et al* (37) reported that YTHDF2-mediated m6A modification of LINC00659, along with the methyltransferase ALKBH5, promoted gastric cancer progression. Similarly, lncRNA LINC00470 has been shown to enhance the YTHDF2-mediated degradation of PTEN mRNA, further causing cancer malignancy (38). These studies implied a promoting role for YTHDF2 in gastric cancer development, consistent with the present findings that the expression of YTHDF2 was increased in gastric cancer cells. However, YTHDF2 has also been implicated in tumor suppression in other studies. Shen *et al* (39) discovered that YTHDF2 inhibited gastric cancer cell proliferation through the forkhead box protein C2 signaling pathway. Additionally, Zhou *et al* (40) reported that the downregulated expression of YTHDF2 promoted gastric cancer progression, suggesting its function as a tumor suppressor. These contrasting findings highlight the dual role of YTHDF2 in cancer and underscore the need for further investigation into the conditions under which YTHDF2 acts as an oncogene or a tumor suppressor.

In the present study, a novel interaction between YTHDF2 and AC026691.1 was detected in gastric cancer cells. Knocking down YTHDF2 alone significantly inhibited the malignant behaviors of gastric cancer cells, including proliferation, migration and EMT, aligning with its proposed oncogenic role. Conversely, knocking down AC026691.1 alone resulted in increased malignancy, suggesting that AC026691.1 may act as a tumor suppressor. The double knockdown of YTHDF2 and AC026691.1 markedly reduced the effects observed with respective knockdowns, indicating a complex interplay between these two molecules in regulating gastric cancer cell behavior. Notably, to the best of our knowledge, the current study was the first to reveal an association between AC026691.1 and EMT in gastric cancer. EMT is a crucial process in cancer metastasis, and in this study, it was indicated that YTHDF2-mediated degradation of AC026691.1 could promote EMT, thereby enhancing cancer cell migration and invasion. These results are consistent with findings from other studies showing that YTHDF2 modulates EMT markers, such as N-cadherin, E-cadherin and MMPs, which are key

regulators of cellular migration and invasion (35,41). For example, PRMT6-mediated YTHDF2 has been shown to influence the Wnt/β-catenin signaling pathway, which regulates N-cadherin and E-cadherin expression in glioblastoma (41). These studies suggested that YTHDF2 may similarly regulate EMT markers and related pathways in gastric cancer, further implicating its role in tumor progression. Future studies should explore whether AC026691.1 degradation by YTHDF2 directly interacts with these signaling pathways to modulate EMT.

Notably, the role of YTHDF2 in macrophage polarization represents a novel feature of its regulatory effects. The conditioned medium from YTHDF2-knockdown gastric cancer cells significantly reduced the proportion of CD206-positive (M2) macrophages while increasing CD80-positive (M1) macrophages. These findings indicated that YTHDF2-mediated degradation of AC026691.1 may enhance the secretion of cytokines or other factors that drive immune suppression. Previous studies have shown that other m6A-modified lncRNAs, such as ZFAS1 and LINC01569, similarly mediate M2 macrophage polarization through cytokine pathways, including IL-10 and Arg-1 (13,42). These findings highlight the complex interplay between YTHDF2, AC026691.1, and immune signaling pathways, further emphasizing the need for detailed exploration of their roles in shaping the tumor microenvironment.

The present findings are consistent with and expand upon the existing literature on YTHDF2 and its role in gastric cancer. It is well-documented that YTHDF2 has dual functions in cancer, acting as both an oncogene and a tumor suppressor under different conditions. However, the current study uniquely positioned AC026691.1 within this context, providing evidence that YTHDF2-mediated degradation of AC026691.1 may contribute to gastric cancer progression. This interaction not only reinforced the oncogenic role of YTHDF2 but also introduced AC026691.1 as a potential tumor suppressor and therapeutic target. Given the growing interest in m6A-targeted therapies, such as inhibitors of methyltransferases or m6A readers, targeting the YTHDF2-AC026691.1 axis may represent a novel therapeutic approach. Further exploration of this axis in preclinical and clinical models is warranted to validate its therapeutic potential and to elucidate its broader implications in the tumor microenvironment.

The present study provided significant insights into the role of AC026691.1 and YTHDF2 in gastric cancer (Fig. 7). The interaction between these molecules, and their impact on EMT and cancer cell behavior underscore the complexity of cancer progression mechanisms. However, the study did not assess the expression levels of YTHDF2 and AC026691.1 in clinical samples, nor did it investigate the impact of YTHDF2-mediated degradation of AC026691.1 on the tumorigenic ability of gastric cancer cells through *in vivo* experiments. Further experimental exploration is needed to understand the mechanisms by which gastric cancer cells initiate YTHDF2-mediated m6A modification of AC026691.1 and their specific effects on macrophages.

In conclusion, the present study demonstrated that YTHDF2 could mediate the degradation of AC026691.1, thereby promoting gastric cancer cell viability, colony formation, migration and EMT, as well as regulating M2 macrophage polarization induced by gastric cancer cells. These findings provide novel insights into the role of YTHDF2 in m6A-regulated lncRNA networks and highlight YTHDF2 as a potential therapeutic target in gastric cancer.

Acknowledgements

Not applicable.

Funding

The present study was supported by the Jiangsu Province Traditional Chinese Medicine Science and Technology Development Program (grant no. YB2020067).

Availability of data and materials

The data generated in the present study may be requested from the corresponding author.

Authors' contributions

CJ and ZW designed the study. JJ and XY collated the data, carried out data analyses and produced the initial draft of the manuscript. ZW validated the experimental results and contributed to drafting the manuscript. CJ and ZW confirm the authenticity of all the raw data. All authors read and approved the final version of the manuscript.

Ethics approval and consent to participate

Not applicable.

Patient consent for publication

Not applicable.

Competing interests

The authors declare that they have no competing interests.

References

1. Mehta SL, Arruri V and Vemuganti R: Role of transcription factors, noncoding RNAs, epitranscriptomics, and epigenetics in post-ischemic neuroinflammation. J Neurochem 168: 3430-3448, 2024.
2. Zhu GM, Chen SQ, Jiang QG, Cao Y, Guo Y and Ye LQ: MiR-216b inhibits gastric cancer proliferation and migration by targeting PARK7. Indian J Pathol Microbiol 64: 52-57, 2021.
3. Dai ZT, Xiang Y, Duan YY, Wang J, Li JP, Zhang HM, Cheng C, Wang Q, Zhang TC and Liao XH: MiR-17-5p and MKL-1 modulate stem cell characteristics of gastric cancer cells. Int J Biol Sci 17: 2278-2293, 2021.
4. Xin L, Liu L, Liu C, Zhou LQ, Zhou Q, Yuan YW, Li SH and Zhang HT: DNA-methylation-mediated silencing of miR-7-5p promotes gastric cancer stem cell invasion via increasing Smo and Hes1. J Cell Physiol 235: 2643-2654, 2020.
5. Lu RH, Xiao ZQ, Zhou JD, Yin CQ, Chen ZZ, Tang FJ and Wang SH: MiR-199a-5p represses the stemness of cutaneous squamous cell carcinoma stem cells by targeting Sirt1 and CD44ICD cleavage signaling. Cell Cycle 19: 1-14, 2020.
6. Miao L, Qi J, Zhao Q, Wu QN, Wei DL, Wei XL, Liu J, Chen J, Zeng ZL, Ju HQ, *et al*: Targeting the STING pathway in tumor-associated macrophages regulates innate immune sensing of gastric cancer cells. Theranostics 10: 498-515, 2020.

7. Zhan P, Shu X, Chen M, Sun L, Yu L, Liu J, Sun L, Yang Z and Ran Y: miR-98-5p inhibits gastric cancer cell stemness and chemoresistance by targeting branched-chain aminotransferases 1. Life Sci 276: 119405, 2021.
8. Wei L, Sun J, Zhang N, Zheng Y, Wang X, Lv L, Liu J, Xu Y, Shen Y and Yang M: Noncoding RNAs in gastric cancer: Implications for drug resistance. Mol Cancer 19: 62, 2020.
9. Yang H, Hu Y, Weng M, Liu X, Wan P, Hu Y, Ma M, Zhang Y, Xia H and Lv K: Hypoxia inducible lncRNA-CBSLR modulates ferroptosis through m6A-YTHDF2-dependent modulation of CBS in gastric cancer. J Adv Res 37: 91-106, 2021.
10. Luo Y, Zheng S, Wu Q, Wu J, Zhou R, Wang C, Wu Z, Rong X, Huang N, Sun L, *et al*: Long noncoding RNA (lncRNA) EIF3J-DT induces chemoresistance of gastric cancer via autophagy activation. Autophagy 17: 4083-4101, 2021.
11. Yang A, Liu X, Liu P, Feng Y, Liu H, Gao S, Huo L, Han X, Wang J and Kong W: LncRNA UCA1 promotes development of gastric cancer via the miR-145/MYO6 axis. Cell Mol Biol Lett 26: 33, 2021.
12. Xu J, Wang X, Zhu C and Wang K: A review of current evidence about lncRNA MEG3: A tumor suppressor in multiple cancers. Front Cell Dev Biol 10: 997633, 2022.
13. Xin L, Wu Y, Liu C, Zeng F, Wang JL, Wu DZ, Wu JP, Yue ZQ, Gan JH, Lu H, *et al*: Exosome-mediated transfer of lncRNA HCG18 promotes M2 macrophage polarization in gastric cancer. Mol Immunol 140: 196-205, 2021.
14. Li C, Chen Z, Gao J, Tang T, Zhou L, Zhang G, Zhang D, Shen C, Guo L and Fu T: MIR4435-2HG in exosomes promotes gastric carcinogenesis by inducing M2 polarization in macrophages. Front Oncol 12: 1017745, 2022.
15. Liu H, Xu Y, Yao B, Sui T, Lai L and Li Z: A novel N6-methyladenosine (m6A)-dependent fate decision for the lncRNA THOR. Cell Death Dis 11: 613, 2020.
16. Wang H, Meng Q and Ma B: Characterization of the prognostic m6A-related lncRNA signature in gastric cancer. Front Oncol 11: 630260, 2021.
17. Zhang C, Zhang M, Ge S, Huang W, Lin X, Gao J, Gong J and Shen L: Reduced m6A modification predicts malignant phenotypes and augmented Wnt/PI3K-Akt signaling in gastric cancer. Cancer Med 8: 4766-4781, 2019.
18. Kassambara A, Kosinski M and Biecek P: survminer: Drawing survival curves using 'ggplot2'. CRAN: Contributed Packages, 2016.
19. Tay JK, Narasimhan B and Hastie T: Elastic net regularization paths for all generalized linear models. J Stat Softw 106: 1, 2023.
20. Zheng J, Dou R, Zhang X, Zhong B, Fang C, Xu Q, Di Z, Huang S, Lin Z, Song J, *et al*: LINC00543 promotes colorectal cancer metastasis by driving EMT and inducing the M2 polarization of tumor associated macrophages. J Transl Med 21: 153, 2023.
21. Qiu S, Xie L, Lu C, Gu C, Xia Y, Lv J, Xuan Z, Fang L, Yang J, Zhang L, *et al*: Gastric cancer-derived exosomal miR-519a-3p promotes liver metastasis by inducing intrahepatic M2-like macrophage-mediated angiogenesis. J Exp Clin Cancer Res 41: 296, 2022.
22. Thrift AP and El-Serag HB: Burden of gastric cancer. Clin Gastroenterol Hepatol 18: 534-542, 2020.
23. Cusenza VY, Tameni A, Neri A and Frazzi R: The lncRNA epigenetics: The significance of m6A and m5C lncRNA modifications in cancer. Front Oncol 13: 1063636, 2023.
24. Zhou L, Li J, Liao M, Zhang Q and Yang M: LncRNA MIR155HG induces M2 macrophage polarization and drug resistance of colorectal cancer cells by regulating ANXA2. Cancer Immunol Immunother 71: 1075-1091, 2022.
25. Barbieri I and Kouzarides T: Role of RNA modifications in cancer. Nat Rev Cancer 20: 303-322, 2020.
26. Sexton RE, Al Hallak MN, Diab M and Azmi AS: Gastric cancer: A comprehensive review of current and future treatment strategies. Cancer Metastasis Rev 39: 1179-1203, 2020.
27. Akhtar J, Lugoboni M and Junion G: m6A RNA modification in transcription regulation. Transcription 12: 266-276, 2021.
28. Ru W, Zhang X, Yue B, Qi A, Shen X, Huang Y, Lan X, Lei C and Chen H: Insight into m^6A methylation from occurrence to functions. Open Biol 10: 200091, 2020.
29. Wan W, Ao X, Chen Q, Yu Y, Ao L, Xing W, Guo W, Wu X, Pu C, Hu X, *et al*: METTL3/IGF2BP3 axis inhibits tumor immune surveillance by upregulating N^6-methyladenosine modification of PD-L1 mRNA in breast cancer. Mol Cancer 21: 60, 2022.
30. Du A, Li S, Zhou Y, Disoma C, Liao Y, Zhang Y, Chen Z, Yang Q, Liu P, Liu S, *et al*: M6A-mediated upregulation of circMDK promotes tumorigenesis and acts as a nanotherapeutic target in hepatocellular carcinoma. Mol Cancer 21: 109, 2022.
31. He PC and He C: m^6 A RNA methylation: From mechanisms to therapeutic potential. EMBO J 40: e105977, 2021.
32. Selmi T and Lanzuolo C: Driving chromatin organisation through N6-methyladenosine modification of RNA: What Do we know and what lies ahead? Genes (Basel) 13: 340, 2022.
33. Yu ZL and Zhu ZM: N6-methyladenosine related long non-coding RNAs and immune cell infiltration in the tumor microenvironment of gastric cancer. Biol Proced Online 23: 15, 2021.
34. Han T, Xu D, Zhu J, Li J, Liu L and Deng Y: Identification of a robust signature for clinical outcomes and immunotherapy response in gastric cancer: Based on N6-methyladenosine related long noncoding RNAs. Cancer Cell Int 21: 432, 2021.
35. Zhang C, Huang S, Zhuang H, Ruan S, Zhou Z, Huang K, Ji F, Ma Z, Hou B and He X: YTHDF2 promotes the liver cancer stem cell phenotype and cancer metastasis by regulating OCT4 expression via m6A RNA methylation. Oncogene 39: 4507-4518, 2020.
36. Zhang M, Wang J, Jin Y, Zheng Q, Xing M, Tang Y, Ma Y, Li L, Yao B, Wu H and Ma C: YTHDF2-mediated FGF14-AS2 decay promotes osteolytic metastasis of breast cancer by enhancing RUNX2 mRNA translation. Br J Cancer 127: 2141-2153, 2022.
37. Fang Y, Wu X, Gu Y, Shi R, Yu T, Pan Y, Zhang J, Jing X, Ma P and Shu Y: LINC00659 cooperated with ALKBH5 to accelerate gastric cancer progression by stabilising JAK1 mRNA in an m^6 A-YTHDF2-dependent manner. Clin Transl Med 13: e1205, 2023.
38. Yan J, Huang X, Zhang X, Chen Z, Ye C, Xiang W and Huang Z: LncRNA LINC00470 promotes the degradation of PTEN mRNA to facilitate malignant behavior in gastric cancer cells. Biochem Biophys Res Commun 521: 887-893, 2020.
39. Shen X, Zhao K, Xu L, Cheng G, Zhu J, Gan L, Wu Y and Zhuang Z: YTHDF2 inhibits gastric cancer cell growth by regulating FOXC2 signaling pathway. Front Genet 11: 592042, 2020.
40. Zhou Y, Fan K, Dou N, Li L, Wang J, Chen J, Li Y and Gao Y: YTHDF2 exerts tumor-suppressor roles in gastric cancer via up-regulating PPP2CA independently of m^6A modification. Biol Proced Online 25: 6, 2023.
41. Yu P, Xu T, Ma W, Fang X, Bao Y, Xu C, Huang J, Sun Y and Li G: PRMT6-mediated transcriptional activation of ythdf2 promotes glioblastoma migration, invasion, and emt via the wnt-β-catenin pathway. J Exp Clin Cancer Res 43: 116, 2024.
42. Ma B, Wang J and Yusufu P: Tumor-derived exosome ElNF1-AS1 affects the progression of gastric cancer by promoting M2 polarization of macrophages. Environ Toxicol 38: 2228-2239, 2023.